

## CHAPTER 5

# A NEW DIFFERENCE SCHEME FOR TIME FRACTIONAL TELEGRAPH EQUATION

In this chapter, we developed a new difference scheme for the time-fractional telegraph equation. This chapter is structured as follows: In section 5.2, approximation of Caputo derivatives of order  $\alpha \in (0, 1)$  and  $(1, 2)$  by the L123 approximation and the L3 approximation respectively is given. In order to solve the TFWWE, a new difference method is proposed in Section 5.3. Four numerical examples is given in Section 5.4 to validate the accuracy of the scheme. Finally, the chapter is concluded in Section 5.5.

## 5.1 Introduction

In this manuscript, we consider the following time-fractional telegraph equation [174]

$$\begin{cases} {}_0^C D_t^\alpha \mathfrak{U}(x, t) + \gamma_1 {}_0^C D_t^\beta \mathfrak{U}(x, t) + \gamma_2 \mathfrak{U}(x, t) = \gamma_3 \mathfrak{U}_{xx}(x, t) + f(x, t), & (x, t) \in \Omega = [x_l, x_r] \times [0, T], \\ I.C. : \mathfrak{U}(x, 0) = \phi_1(x), \quad \partial_t \mathfrak{U}(x, 0) = \phi_2(x); \\ B.C. : \mathfrak{U}(x_l, t) = \psi_1(x), \quad \mathfrak{U}(x_r, t) = \psi_2(x). \end{cases} \quad (5.1)$$

where,  $1 < \alpha < 2$  and  $0 < \beta < 1$  and the Caputo fractional derivatives is defined as

$${}_0^C D_t^\beta \mathfrak{U}(\cdot, t) = \frac{1}{\Gamma(1 - \beta)} \int_0^t \frac{\mathfrak{U}'(\cdot, s)}{(t - s)^\beta} ds, \quad \beta \in (0, 1), \quad (5.2)$$

$${}_0^C D_t^\alpha \mathfrak{U}(\cdot, t) = \frac{1}{\Gamma(2 - \alpha)} \int_0^t \frac{\mathfrak{U}''(\cdot, s)}{(t - s)^{\alpha-1}} ds, \quad \alpha \in (1, 2). \quad (5.3)$$

### 5.1.1 Our contribution

The following points explains the main contributions of this chapter:

- We have applied two numerical approximations for the Caputo derivative of order  $\alpha$  i.e. L3 approximation [175] for  $\alpha \in (1, 2)$  and L123 approximation [106] for  $\beta \in (0, 1)$ .
- A difference scheme is proposed by using these two approximation in combination with central difference approximation for space derivatives. In order to validate the accuracy of our scheme, four test examples of the TFWEs are provided.

- In comparison to the preceding scheme given in [3], it is found that the presented scheme performs significantly improved in terms of accuracy and order.
- In a computational framework, the order of convergence of the proposed difference scheme is  $\mathcal{O}(\tau^2, h^2)$ .

To the best of our knowledge, this is the first time the proposed approach has been implemented for any TFTE. Stability and convergence of the proposed scheme is under investigation.

## 5.2 Time discretization

This section includes the L3 and L123 approximation of order  $\alpha \in (1, 2)$  and  $\beta \in (0, 1)$  of the Caputo derivative, respectively.

### 5.2.1 L3 approximation of the Caputo derivative of order

$$\alpha \in (1, 2)$$

The Caputo fractional derivative of order  $\alpha \in (1, 2)$  is defined as:

$${}_0^C D_t^\alpha \mathfrak{U}(t)|_{t=t_k} = \frac{1}{\Gamma(2-\alpha)} \int_{t_0}^{t_k} \frac{\mathfrak{U}''(s)}{(t_k-s)^{\alpha-1}} ds,$$

We have applied the newly developed L3 approximation [175] of discretizing the Caputo time fractional derivative of order  $\alpha \in (1, 2)$ . Let  $\{t_k = k\tau, k = 0, 1, 2, \dots, N_t\}$  with step length  $\tau = T/N_t$  where,  $N_t$  denotes the temporal discretization parameter,

then the L3 approximation is defined as:

$${}_0\mathbb{D}_t^\alpha \mathfrak{U}(t_k) = \frac{\tau^{-\alpha}}{\Gamma(3-\alpha)} \sum_{j=0}^{k-1} \mathfrak{c}_{k-j-1}^{(k,\alpha)} \Delta^2 \mathfrak{U}_{j-1}. \quad (5.4)$$

The coefficients  $\mathfrak{a}_j^{(\alpha)}$ ,  $\mathfrak{b}_j^{(\alpha)}$  and  $\mathfrak{c}_j^{(k,\alpha)}$  for  $0 \leq j \leq k-1$  is defined as,

$$\mathfrak{a}_j^{(\alpha)} = (j+1)^{2-\alpha} - j^{2-\alpha}, \quad (5.5)$$

$$\mathfrak{b}_j^{(\alpha)} = \frac{1}{(3-\alpha)} \{(j+1)^{3-\alpha} - j^{3-\alpha}\} + (j+1)^{2-\alpha} - 2j^{2-\alpha}. \quad (5.6)$$

for  $k = 1$ ,

$$\mathfrak{c}_0^{(k,\alpha)} = 1,$$

for  $k = 2$ ,

$$\mathfrak{c}_j^{(k,\alpha)} = \begin{cases} -\mathfrak{a}_1^{(\alpha)} + \mathfrak{b}_0^{(\alpha)} + \mathfrak{b}_1^{(\alpha)}, & j = 0, \\ \mathfrak{a}_0^{(\alpha)} + 2\mathfrak{a}_1^{(\alpha)} - \mathfrak{b}_0^{(\alpha)} - \mathfrak{b}_1^{(\alpha)}, & j = 1, \end{cases} \quad (5.7)$$

for  $k = 3$ ,

$$\mathfrak{c}_j^{(k,\alpha)} = \begin{cases} \mathfrak{b}_0^{(\alpha)} & j = 0, \\ \mathfrak{a}_0^{(\alpha)} - \mathfrak{a}_2^{(\alpha)} - \mathfrak{b}_0^{(\alpha)} + \mathfrak{b}_1^{(\alpha)} + \mathfrak{b}_2^{(\alpha)}, & j = 1, \\ \mathfrak{a}_1^{(\alpha)} + 2\mathfrak{a}_2^{(\alpha)} - \mathfrak{b}_1^{(\alpha)} - \mathfrak{b}_2^{(\alpha)}, & j = 2, \end{cases} \quad (5.8)$$

for  $k \geq 4$ ,

$$\mathbf{c}_j^{(k,\alpha)} = \begin{cases} \mathbf{b}_0^{(\alpha)} & j = 0, \\ \mathbf{a}_{j-1}^{(\alpha)} - \mathbf{b}_{j-1}^{(\alpha)} + \mathbf{b}_j^{(\alpha)} & 1 \leq j \leq k-3, \\ \mathbf{a}_{k-3}^{(\alpha)} - \mathbf{a}_{k-1}^{(\alpha)} - \mathbf{b}_{k-3}^{(\alpha)} + \mathbf{b}_{k-2}^{(\alpha)} + \mathbf{b}_{k-1}^{(\alpha)}, & j = k-2, \\ \mathbf{a}_{k-2}^{(\alpha)} + 2\mathbf{a}_{k-1}^{(\alpha)} - \mathbf{b}_{k-2}^{(\alpha)} - \mathbf{b}_{k-1}^{(\alpha)}, & j = k-1. \end{cases} \quad (5.9)$$

**Theorem 5.2.1.** The truncation error in L3 approximation is given by,

$${}_0^C D_t^\alpha \mathfrak{U}(t)|_{t=t_k} - {}_0 \mathbb{D}_t^\alpha \mathfrak{U}(t_k) = \mathcal{O}(\tau^2). \quad (5.10)$$

*Proof.* The proof follows [175]. □

## 5.2.2 L123 approximation of the Caputo derivative of order $\beta \in (0, 1)$

The Caputo fractional derivative of order  $\beta \in (0, 1)$  is defined as:

$${}_0^C D_t^\beta \mathfrak{U}(t)|_{t=t_k} = \frac{1}{\Gamma(1-\beta)} \int_{t_0}^{t_k} \frac{\mathfrak{U}'(s)}{(t_k - s)^\beta} ds.$$

The L123 approximation [106] of the Caputo derivative of order  $\beta \in (0, 1)$  is defined as:

$$\tilde{\mathbb{D}}_t^\beta \mathfrak{U}(t)|_{t=t_k} = \frac{\tau^{-\beta}}{\Gamma(2-\beta)} \left( \mathbf{e}_0^\beta \mathfrak{U}(t_k) - \sum_{j=1}^{k-1} (\mathbf{e}_{k-j-1}^\beta - \mathbf{e}_{k-j}^\beta) \mathfrak{U}(t_j) - \mathbf{e}_{k-1}^\beta \mathfrak{U}(t_0) \right). \quad (5.11)$$

The coefficients  $\bar{\alpha}_j^{(\beta)}$ ,  $\bar{\mathbf{b}}_j^{(\beta)}$  and  $\bar{\mathbf{c}}_j^{(k,\beta)}$  is defined for  $j \in [0, k-1]$  as,

$$\bar{\alpha}_j^{(\beta)} = (j+1)^{1-\beta} - j^{1-\beta}, \quad (5.12)$$

$$\bar{\mathbf{b}}_j^{(\beta)} = \frac{1}{(2-\beta)} \{(j+1)^{2-\beta} - j^{2-\beta}\} - \frac{1}{2} \{(j+1)^{1-\beta} + j^{1-\beta}\}, \quad (5.13)$$

$$\bar{\mathbf{c}}_j^{(\beta)} = \frac{1}{(2-\beta)(3-\beta)} \{(j+1)^{3-\beta} - j^{3-\beta}\} - \frac{1}{(2-\beta)} j^{2-\beta} - \frac{1}{6} \{(j+1)^{1-\beta} + 2j^{1-\beta}\}, \quad (5.14)$$

where, for  $k=1$ ,  $\mathbf{e}_0^\beta = 1$ ;

for  $k=2$ ,  $\mathbf{e}_0^\beta = \bar{\alpha}_0^\beta + \bar{\mathbf{b}}_0^\beta \in (1, 1.5)$ ,  $\mathbf{e}_1^\beta = \bar{\alpha}_1^\beta - \bar{\mathbf{b}}_0^\beta \in (-0.5, 1)$ ;

for  $k=3$ ,

$$\mathbf{e}_j^{(\beta)} = \begin{cases} \bar{\alpha}_j^{(\beta)} + \bar{\mathbf{b}}_j^{(\beta)} + \bar{\mathbf{c}}_j^{(\beta)}, & j=0, \\ \bar{\alpha}_j^{(\beta)} + \bar{\mathbf{b}}_j^{(\beta)} - \bar{\mathbf{b}}_{j-1}^{(\beta)} - 2\bar{\mathbf{c}}_{j-1}^{(\beta)}, & j=1, \\ \bar{\alpha}_j^{(\beta)} - \bar{\mathbf{b}}_{j-1}^{(\beta)} + \bar{\mathbf{c}}_{j-2}^{(\beta)}, & j=2. \end{cases} \quad (5.15)$$

Here,  $\mathbf{e}_0^{(\beta)} \in (1, 11/6)$ ,  $\mathbf{e}_1^{(\beta)} \in (-7/6, 1)$ , and  $\mathbf{e}_2^{(\beta)} \in (0, 1)$ .

For  $k \geq 4$ ,

$$\mathbf{e}_j^{(\beta)} = \begin{cases} \bar{\alpha}_j^{(\beta)} + \bar{\mathbf{b}}_j^{(\beta)} + \bar{\mathbf{c}}_j^{(\beta)}, & j=0, \\ \bar{\alpha}_j^{(\beta)} + \bar{\mathbf{b}}_j^{(\beta)} - \bar{\mathbf{b}}_{j-1}^{(\beta)} + \bar{\mathbf{c}}_j^{(\beta)} - 2\bar{\mathbf{c}}_{j-1}^{(\beta)}, & j=1, \\ \bar{\alpha}_j^{(\beta)} + \bar{\mathbf{b}}_j^{(\beta)} - \bar{\mathbf{b}}_{j-1}^{(\beta)} + \bar{\mathbf{c}}_j^{(\beta)} - 2\bar{\mathbf{c}}_{j-1}^{(\beta)} + \bar{\mathbf{c}}_{j-2}^{(\beta)}, & 2 \leq j \leq k-3, \\ \bar{\alpha}_j^{(\beta)} + \bar{\mathbf{b}}_j^{(\beta)} - \bar{\mathbf{b}}_{j-1}^{(\beta)} - 2\bar{\mathbf{c}}_{j-1}^{(\beta)} + \bar{\mathbf{c}}_{j-2}^{(\beta)}, & j=k-2, \\ \bar{\alpha}_j^{(\beta)} - \bar{\mathbf{b}}_{j-1}^{(\beta)} + \bar{\mathbf{c}}_{j-2}^{(\beta)}, & j=k-1. \end{cases} \quad (5.16)$$

### 5.3 Numerical scheme for TFTE

Let  $\{x_i = x_l + ih, i = 0, 1, 2, \dots, M_x\}$  and  $\{t_k = k\tau, k = 0, 1, 2, \dots, N_t\}$  be the uniform meshes with step lengths  $h = (x_r - x_l)/M_x$  and  $\tau = T/N_t$  where  $M_x$  and  $N_t$  are the discretization parameters in  $x$  and  $t$ , respectively. The TFTE at each discrete point  $(x_i, t_k)$  can be written as:

$${}_0^C D_t^\alpha \mathfrak{U}(x_i, t_k) + \gamma_{10} {}_0^C D_t^\beta \mathfrak{U}(x_i, t_k) + \gamma_2 \mathfrak{U}(x_i, t_k) = \gamma_3 \frac{\partial^2 \mathfrak{U}(x_i, t_k)}{\partial x^2} + f(x_i, t_k), \quad (5.17)$$

with initial conditions

$$\mathfrak{U}(x_i, 0) = \phi_1(x_i), \quad \partial_t \mathfrak{U}(x_i, 0) = \phi_2(x_i), \quad (5.18)$$

and boundary conditions

$$\mathfrak{U}(x_l, t_k) = \psi_1(t_k), \quad \mathfrak{U}(x_r, t_k) = \psi_2(t_k). \quad (5.19)$$

For the first time level  $t_1$ , applying L3 an L123 approximation in fractional time derivative and central difference scheme for space derivative in (5.17), we have

$$\mathbb{D}_t^\alpha \mathfrak{U}(x_i, t_1) + \gamma_1 \tilde{\mathbb{D}}_t^\beta \mathfrak{U}(x_i, t_1) + \gamma_2 \mathfrak{U}(x_i, t_1) = \gamma_3 \frac{\partial^2 \mathfrak{U}(x_i, t_1)}{\partial x^2} + f(x_i, t_1), \quad (5.20)$$

$$\frac{\tau^{-\alpha}}{\Gamma(3-\alpha)} (\mathfrak{U}_i^1 - 2\mathfrak{U}_i^0 + \mathfrak{U}_i^{-1}) + \gamma_1 \frac{\tau^{-\beta}}{\Gamma(2-\beta)} (\mathfrak{U}_i^1 - \mathfrak{U}_i^0) + \gamma_2 \mathfrak{U}_i^1 = \frac{\gamma_3}{h^2} (\mathfrak{U}_{i+1}^1 - 2\mathfrak{U}_i^1 + \mathfrak{U}_{i-1}^1) + f_i^1. \quad (5.21)$$

Since,  $\partial_t \mathfrak{U}(x_i, 0) = \phi_2(x_i)$  therefore,

$$\frac{\mathfrak{U}_i^1 - \mathfrak{U}_i^{-1}}{2\tau} = \phi_2(x_i), \quad (5.22)$$

$$\mathfrak{U}_i^{-1} = \mathfrak{U}_i^1 - 2\tau\phi_2(x_i). \quad (5.23)$$

Let  $\mu^{(\alpha)} = \frac{\tau^{-\alpha}}{\Gamma(3-\alpha)}$  and  $\mu^{(\beta)} = \frac{\tau^{-\beta}}{\Gamma(2-\beta)}$ . Now, rearranging the terms, we get

$$\mu^{(\alpha)}(-2\mathfrak{U}_i^0 + \mathfrak{U}_i^{-1}) + \gamma_1\mu^{(\beta)}(-\mathfrak{U}_i^0) - \mathfrak{f}_i^1 = \frac{\gamma_3}{h^2}\mathfrak{U}_{i+1}^1 - \left(\frac{2\gamma_3}{h^2} + \mu^{(\alpha)} + \gamma_1\mu^{(\beta)} + \gamma_2\right)\mathfrak{U}_i^1 + \frac{\gamma_3}{h^2}\mathfrak{U}_{i-1}^1. \quad (5.24)$$

From the boundary conditions, we can get  $\mathfrak{U}_0^1 = \psi_1(\mathbf{t}_1)$  and  $\mathfrak{U}_M^1 = \psi_2(\mathbf{t}_k)$ . Therefore, the discrete form of TFWE at time level  $\mathbf{t}_k$  for  $k \geq 2$  is

$$\mathbb{D}_t^\alpha \mathfrak{U}(x_i, \mathbf{t}_k) + \gamma_1 \tilde{\mathbb{D}}_t^\beta \mathfrak{U}(x_i, \mathbf{t}_k) + \gamma_2 \mathfrak{U}(x_i, \mathbf{t}_k) = \gamma_3 \frac{\partial^2 \mathfrak{U}(x_i, \mathbf{t}_k)}{\partial X^2} + \mathfrak{f}(x_i, \mathbf{t}_k), \quad (5.25)$$

$$\begin{aligned} \mu^{(\alpha)} \left[ \sum_{j=0}^{k-1} \mathbf{c}_{k-j-1}^{(k,\alpha)} \Delta^2 \mathfrak{U}_i^{j-1} \right] + \gamma_1 \mu^{(\beta)} \left[ \mathbf{e}_0^\beta \mathfrak{U}_i^k - \sum_{j=1}^{k-1} (\mathbf{e}_{k-j-1}^\beta - \mathbf{e}_{k-j}^\beta) \mathfrak{U}_i^j - \mathbf{e}_{k-1}^\beta \mathfrak{U}_i^0 \right] + \gamma_2 \mathfrak{U}_i^k \\ = \frac{\gamma_3}{h^2} (\mathfrak{U}_{i+1}^k - 2\mathfrak{U}_i^k + \mathfrak{U}_{i-1}^k) + \mathfrak{f}_i^k, \end{aligned} \quad (5.26)$$

on simplifying, we have,

$$\begin{aligned} \mu^{(\alpha)} \left[ \mathbf{c}_{k-1}^{(k,\alpha)} \mathfrak{U}_i^{-1} + (\mathbf{c}_{k-2}^{(k,\alpha)} - 2\mathbf{c}_{k-1}^{(k,\alpha)}) \mathfrak{U}_i^0 + \sum_{j=2}^{k-1} (\mathbf{c}_{k-j+1}^{(k,\alpha)} - 2\mathbf{c}_{k-j}^{(k,\alpha)} + \mathbf{c}_{k-j-1}^{(k,\alpha)}) \mathfrak{U}_i^{j-1} + (\mathbf{c}_1^{(k,\alpha)} - 2\mathbf{c}_0^{(k,\alpha)}) \mathfrak{U}_i^{k-1} \right] \\ + \gamma_1 \mu^{(\beta)} \left[ - \sum_{j=1}^{k-1} (\mathbf{e}_{k-j-1}^\beta - \mathbf{e}_{k-j}^\beta) \mathfrak{U}_i^j - \mathbf{e}_{k-1}^\beta \mathfrak{U}_i^0 \right] = \frac{\gamma_3}{h^2} \mathfrak{U}_{i+1}^k - \left( \frac{2\gamma_3}{h^2} + \mu^{(\alpha)} \mathbf{c}_0^{(k,\alpha)} + \gamma_1 \mu^{(\beta)} \mathbf{e}_0^{(k,\alpha)} + \gamma_2 \right) \mathfrak{U}_i^k \\ + \frac{\gamma_3}{h^2} \mathfrak{U}_{i-1}^k + \mathfrak{f}_i^k. \end{aligned} \quad (5.27)$$

The matrix form of the scheme (5.27) is given by

$$\left\{ \begin{array}{l} \mathbb{A}_1 \mathbb{U}^1 = -2\mathbb{U}^0 + \mathbb{U}^{-1} - \mathbb{F}^1 + \mathbb{G}^1, \quad \text{for } k = 1, \\ \mathbb{A}_k \mathbb{U}^k = \mu^{(\alpha)} \left[ \mathbf{c}_{k-1}^{(k,\alpha)} \mathbb{U}^{-1} + (\mathbf{c}_{k-2}^{(k,\alpha)} - 2\mathbf{c}_{k-1}^{(k,\alpha)}) \mathbb{U}^0 + \sum_{j=2}^{k-1} (\mathbf{c}_{k-j+1}^{(k,\alpha)} - 2\mathbf{c}_{k-j}^{(k,\alpha)} + \mathbf{c}_{k-j-1}^{(k,\alpha)}) \mathbb{U}^{j-1} \right] \\ \quad + \gamma_1 \mu^{(\beta)} \left[ -\sum_{j=1}^{k-1} (\mathbf{e}_{k-j-1}^\beta - \mathbf{e}_{k-j}^\beta) \mathbb{U}^j - \mathbf{e}_{k-1}^\beta \mathbb{U}^0 \right] \\ \quad + \gamma_2 \mu^{(\alpha)} \left[ (\mathbf{c}_1^{(k,\alpha)} - 2\mathbf{c}_0^{(k,\alpha)}) \mathbb{U}^{k-1} \right] - \mathbb{F}^k + \mathbb{G}^k, \quad \text{for } k \geq 2. \end{array} \right.$$

Where the matrix  $\mathbb{A}_k$ ,  $k = 1, 2, \dots, (N_t - 1)$  is of order  $(N_t - 1)$

$$\mathbb{A}_k = \text{tridiag} \left[ \frac{\gamma_3}{h^2}, -\left( \frac{2\gamma_3}{h^2} + \mu^{(\alpha)} \mathbf{c}_0^{(k,\alpha)} + \gamma_1 \mu^{(\beta)} \mathbf{e}_0 + \gamma_2 \right), \frac{\gamma_3}{h^2} \right], \text{ for } k \geq 1, \quad (5.28)$$

and the vector  $\mathbb{U}^k = [\mathfrak{u}_1^k, \mathfrak{u}_2^k, \dots, \mathfrak{u}_{N_t-1}^k]^T$  be the numerical solution at  $\mathfrak{t}_k$ ,

$$\mathbb{F}^k = [f_1^k, f_2^k, \dots, f_{N_t-1}^k]^T \text{ and } \mathbb{G}^k = \left[ -\frac{\gamma_3}{h^2} \mathfrak{u}_1^0, 0, \dots, 0, -\frac{\gamma_3}{h^2} \mathfrak{u}_1^{M_x} \right]^T.$$

The algorithm for solving TFTE by scheme (5.27) is.

---

**Algorithm 5:** To evaluate the numerical solution of TFTE (5.1)

---

**Input:** The rectangular domain  $\Omega = [0, L] \times [0, T]$ ,  $M_x$ ,  $h = L/M_x$ ,  $N_t$ ,

$\tau = T/N_t$ , initial conditions  $\phi_1(x)$ ,  $\phi_2(x)$ , boundary conditions  $\psi_1(x)$ ,

$\psi_2(x)$  and  $\alpha \in (1, 2)$ ,  $\beta \in (0, 1)$ .

**Output:** The discrete solutions at each grid point  $(x_i, t_k)$

**for** Numerical solution of TFTE by the difference scheme **do**

**Step-1.1** Divide the rectangular domain in uniform step size

$x_i = ih$ ,  $i = 0, 1, \dots, M_x$  and  $t_k = k\tau$ ,  $k = 0, 1, \dots, N_t$ .

**Step-1.2** Apply L123 and L3 approximation (5.4) to discretize the Caputo

fractional derivative in time of order (0,1) and (1,2) respectively and

central difference scheme to discretise the spatial derivatives term.

**Step-1.3** Use initial condition  $\mathfrak{U}(x_i, 0) = \phi_1(x_i)$  and  $\partial_t \mathfrak{U}(x_i, 0) = \phi_2(x_i)$  to

calculate  $\mathfrak{U}_i^0$  and  $\mathfrak{U}_i^{-1}$ , respectively.

**Step-1.4** Use the boundary conditions  $\mathfrak{U}(0, t) = \psi_1(x_i)$  and

$\mathfrak{U}(L, t) = \psi_2(x_i)$  to calculate the values of  $\mathfrak{U}_0^k$  and  $\mathfrak{U}_M^k$ , respectively.

**Step-1.5** The difference scheme for the numerical solution at first time level

$\mathfrak{U}_i^1$  is given in (5.24).

**Step-1.6** Use this solution  $\mathfrak{U}_i^1$  to get the numerical solution  $\mathfrak{U}_i^k$  at time level

$t_k$  for  $k \geq 2$  by the difference scheme (5.27).

**Step-1.7** Repeat Step 1.6 and use all the values of  $\mathfrak{U}_i^k$  at each previous time

levels till we get the discrete solution of TFWE at each discretised points

$(x_i, t_k)$ .

**end**

---

## 5.4 Numerical examples

*Example 5.4.1.* Consider the following TFTE [3] with homogeneous boundary conditions

$$\begin{cases} {}^C_0D_t^\alpha \mathfrak{U}(x, t) + {}^C_0D_t^\beta \mathfrak{U}(x, t) + \mathfrak{U}(x, t) = \frac{\partial^2 \mathfrak{U}(x, t)}{\partial x^2} + f(x, t), & (x, t) \in [0, 1] \times [0, 1] \\ I.C. : \mathfrak{U}(x, 0) = \partial_t \mathfrak{U}(x, 0) = 0, & x \in [0, 1], \\ B.C. : \mathfrak{U}(l, t) = 0, & l = 0, 1, \end{cases} \quad (5.29)$$

with source function

$$f(x, t) = \left( \frac{6t^{3-\alpha}}{\Gamma(4-\alpha)} + \frac{6t^{3-\beta}}{\Gamma(4-\beta)} + t^3 \right) (\sin x)^2 - 2t^3 \cos 2x. \quad (5.30)$$

Exact solution of Ex. 5.4.1 is  $\mathfrak{U}(x, t) = t^3(\sin x)^2$ .

Let  $N_t = 100$  and  $M_x = 100$  then the findings of Ex. 5.4.1 are given as follows:

- Fig. 5.1, 5.2 and 5.3 shows maximum absolute error for  $\alpha = \{1.1, 1.5, 1.9\}$  respectively. It shows that, the numerical solutions attains good accuracy at every time step for all  $\alpha$ .
- Fig. 5.4, 5.5 depicts the absolute error at  $T = 1$  for  $\alpha = 1.75$  in two extended spatial domain, when  $M_x = 100$  and  $N_t = 100$ . It confirms that the proposed method can be credible in the large scale problems.
- The absolute error at  $T = 1$  for various  $\alpha$  is demonstrated in Fig. 5.6.

- The order of convergence (CO) in time w.r.t.  $L_2$  error and  $L_\infty$ -error for  $\alpha = \{1.1, 1.5, 1.9\}$ , at  $T = 1$  is provided in Table 5.1 by taking  $N_t = 10 \times 2^m$ ,  $m = 0, 1, \dots, 5$  and  $M_x = 1000$  grid points.
- Table 5.1 provides the comparative study of the maximum absolute error (MAE) with the results obtained in [3] for  $\alpha = 1.5, 1.9$  at  $T = 1$  by taking  $M_x = 1000$ . It is found that the scheme (5.28) are highly accurate with higher CO for all  $\alpha$  in comparison to [3].
- The CO in space w.r.t.  $L_2$  error and  $L_\infty$ -error for  $\alpha = \{1.1, 1.5, 1.9\}$ , at  $T = 1$  is provided in Table 5.2 by taking  $M_x = 5 \times 2^m$ ,  $m = 0, 1, \dots, 5$  and  $N_t = 1000$  temporal grid points. From both the tables, it can be concluded that the CO of the numerical scheme is  $\mathcal{O}(\tau^2, h^2)$  for all  $\alpha$ .

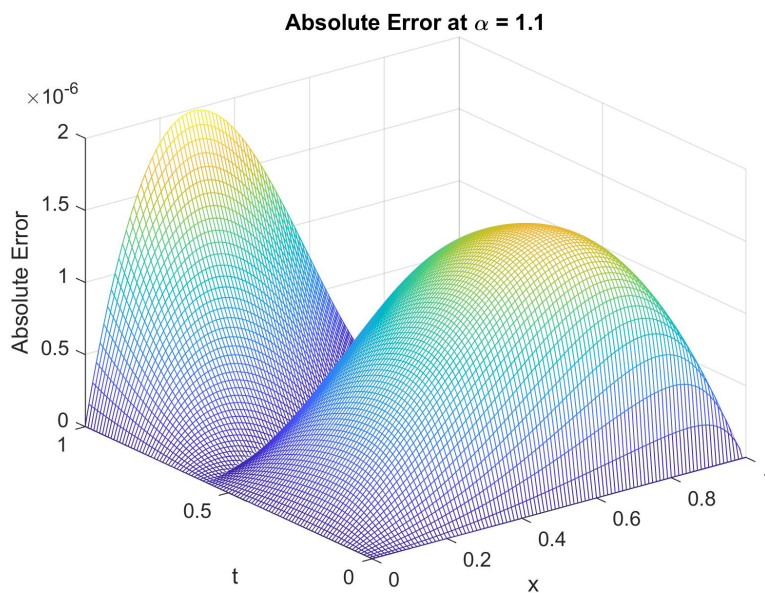


FIGURE 5.1: Graph of the absolute error of Ex. 5.4.1 at  $\alpha = 1.1$ ,  $N_t = 100$ ,  $M_x = 100$ .

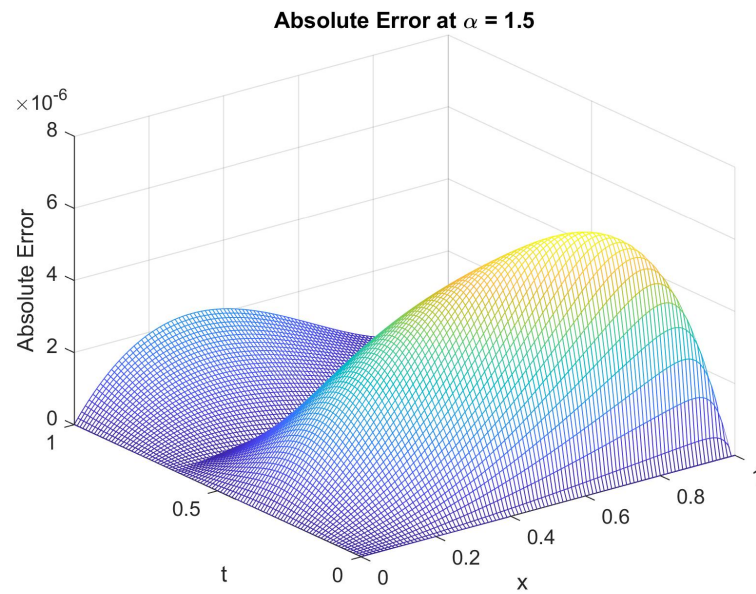


FIGURE 5.2: Graph of the absolute error of Ex. 5.4.1 at  $\alpha = 1.5$ ,  $N_t = 100$ ,  $M_x = 100$ .

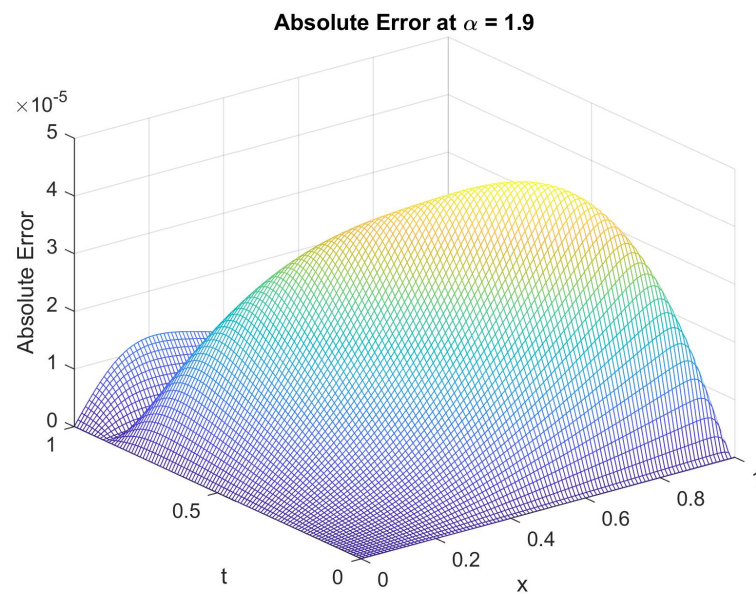


FIGURE 5.3: Graph of the absolute error of Ex. 5.4.1 at  $\alpha = 1.9$ ,  $N_t = 100$ ,  $M_x = 100$ .

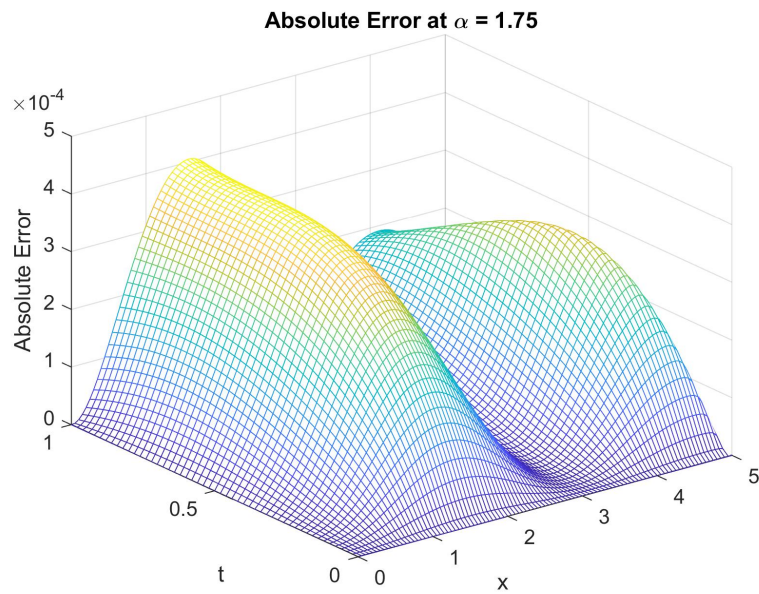


FIGURE 5.4: Graph of the absolute error of Ex. 5.4.1 in an extended domain  $[0,5]$  at  $\alpha = 1.75$ ,  $N_t = 100$ ,  $M_x = 100$ .

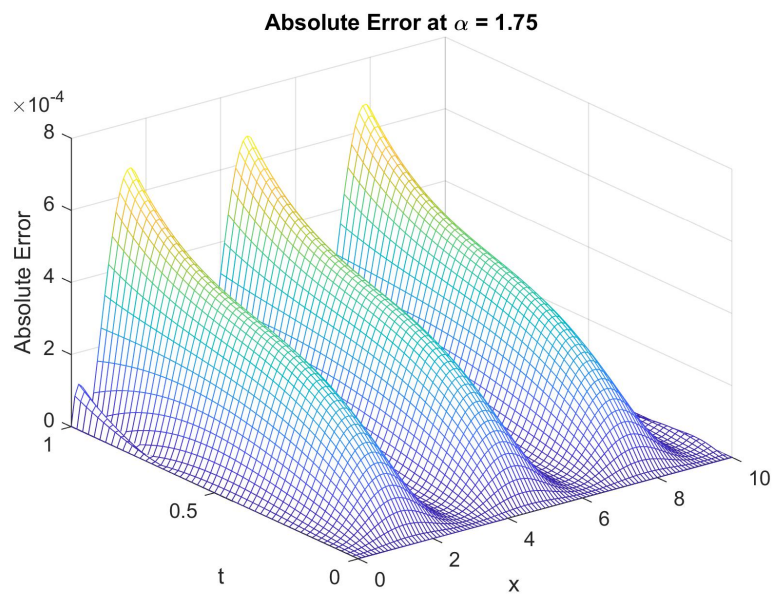


FIGURE 5.5: Graph of the absolute error of Ex. 5.4.1 in an extended domain  $[0,10]$  at  $\alpha = 1.75$ ,  $N_t = 100$ ,  $M_x = 100$ .

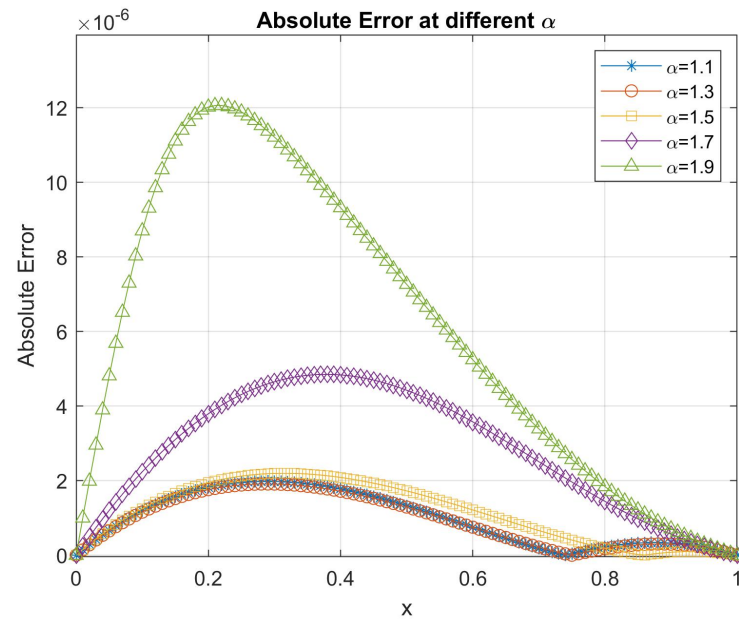


FIGURE 5.6: absolute error of Ex. 5.4.1 at  $T = 1$  for different  $\alpha$ ,  $N_t = 100$ ,  $M_x = 100$ .

$\alpha$	$\tau$	Scheme (5.27)				Kumar et. al.[3]		
		$L_2$ error	order	MAE	CO	$L_2$ error	MAE	CO
<b>1.1</b>	1/10	9.326E-05	-	1.329E-04	-	-	-	-
	1/20	2.416E-05	1.949	3.459E-05	1.942	-	-	-
	1/40	6.037E-06	2.001	8.645E-06	2.000	-	-	-
	1/80	1.486E-06	2.022	2.127E-06	2.023	-	-	-
	1/160	3.565E-07	2.060	5.134E-07	2.051	-	-	-
	1/320	2.635E-08	2.223	1.145E-07	2.165	-	-	-
<b>1.5</b>	1/10	3.243E-05		5.879E-05	-	1.6759E-03	2.3879E-03	-
	1/20	5.084E-06	2.673	9.509E-06	2.628	6.0373E-04	8.6047E-04	1.47
	1/40	1.558E-06	1.707	2.632E-06	1.853	2.1632E-04	3.0834E-04	1.48
	1/80	4.861E-07	1.680	7.620E-07	1.788	7.7184E-05	1.1004E-04	1.49
	1/160	1.343E-07	1.856	2.079E-07	1.874	2.7439E-05	3.9131E-05	1.50
	1/320	2.929E-08	2.197	4.892E-08	2.088	-	-	-
<b>1.9</b>	1/10	7.553E-04		1.315E-03	-	9.8112E-03	1.3760E-02	-
	1/20	3.703E-05	4.350	6.203E-05	4.406	4.7162E-03	6.5907E-03	1.06
	1/40	2.987E-05	0.310	4.974E-05	0.319	2.2348E-03	3.1163E-03	1.08
	1/80	9.336E-06	1.678	1.579E-05	1.655	1.0508E-03	1.4634E-03	1.09
	1/160	2.412E-06	1.953	4.116E-06	1.923	4.9209E-04	6.8491E-04	1.09
	1/320	5.970E-07	2.014	1.035E-06	2.008	-	-	-

TABLE 5.1:  $L_2$  error, MAE with CO in Ex. 5.4.1 for  $\alpha = \{1.1, 1.5, 1.9\}$  at  $T = 1$ ,  $M_x = 500$ .

$\alpha$	h	$L_2$ error		MAE	
		Scheme (5.27)	CO	Scheme (5.27)	CO
<b>1.1</b>	1/5	7.780E-04	0	1.134E-03	0
	1/10	1.955E-04	1.992	2.846E-04	1.995
	1/20	4.893E-05	1.999	7.181E-05	1.987
	1/40	1.223E-05	2.000	1.795E-05	2.000
	1/80	3.051E-06	2.003	4.483E-06	2.001
	1/160	7.565E-07	2.012	1.114E-06	2.009
<b>1.5</b>	1/5	6.469E-04	0	9.465E-04	0
	1/10	1.633E-04	1.986	2.397E-04	1.982
	1/20	4.092E-05	1.997	6.081E-05	1.979
	1/40	1.023E-05	2.000	1.521E-05	2.000
	1/80	2.555E-06	2.001	3.779E-06	2.001
	1/160	6.358E-07	2.007	9.467E-07	2.005
<b>1.9</b>	1/5	4.753E-04	0	6.972E-04	0
	1/10	1.209E-04	1.975	1.850E-04	1.914
	1/20	3.039E-05	1.993	4.649E-05	1.992
	1/40	7.644E-06	1.991	1.170E-05	1.990
	1/80	1.952E-06	1.969	2.993E-06	1.967
	1/160	5.287E-07	1.884	8.131E-07	1.880

TABLE 5.2:  $L_2$  error and MAE with CO in Ex. 5.4.1 for  $\alpha = \{1.1, 1.5, 1.9\}$  at  $T = 1$  with  $N_t = 1000$ .

*Example 5.4.2.* [125] Consider the TFTE

$$\begin{cases} {}_0^C D_t^\alpha \mathfrak{U}(x, t) + {}_0^C D_t^\beta \mathfrak{U}(x, t) + \mathfrak{U}(x, t) = \frac{\partial^2 \mathfrak{U}(x, t)}{\partial x^2} + f(x, t), & (x, t) \in [0, 1] \times [0, \pi] \\ I.C. : \mathfrak{U}(x, 0) = \partial_t \mathfrak{U}(x, 0) = 0, & x \in [0, \pi], \\ B.C. : \mathfrak{U}(l, t) = 0, & l = 0, \pi, \end{cases} \quad (5.31)$$

with the source function

$$f(x, t) = \left( \frac{\Gamma(4 + \beta)}{6} t + \frac{\Gamma(4 + \beta)}{2} + 2t^{1+\beta} \right) t^2 \sin x. \quad (5.32)$$

The exact solution of Ex. 5.4.2 is  $\mathfrak{U}(x, t) = t^{(3+\beta)} \sin x$ . In this example, the absolute error in Ex. 5.4.2, for  $\alpha = 1.2, 1.5$  and  $1.99$  are shown in Fig. 5.7, 5.8, 5.9. The absolute error for distinct values of  $\alpha$  at  $T = 1$  is displayed in Fig. 5.10. The  $L_2$  and  $L_\infty$  error with CO for different values of  $\alpha$  are provided in Table 5.3-5.4 respectively. The example validates the proposed scheme effectiveness.

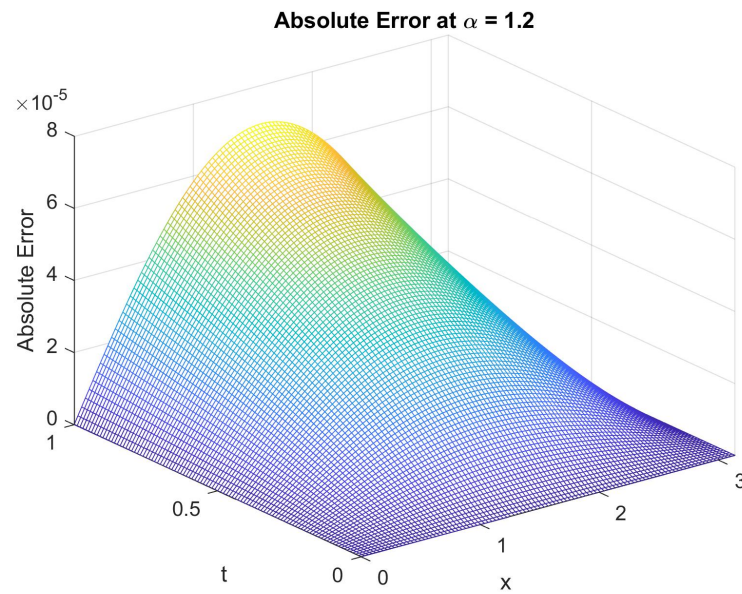


FIGURE 5.7: Graph of the absolute error of Ex. 5.4.2 at  $\alpha = 1.2$ ,  $N_t = 100$ ,  $M_x = 100$ .

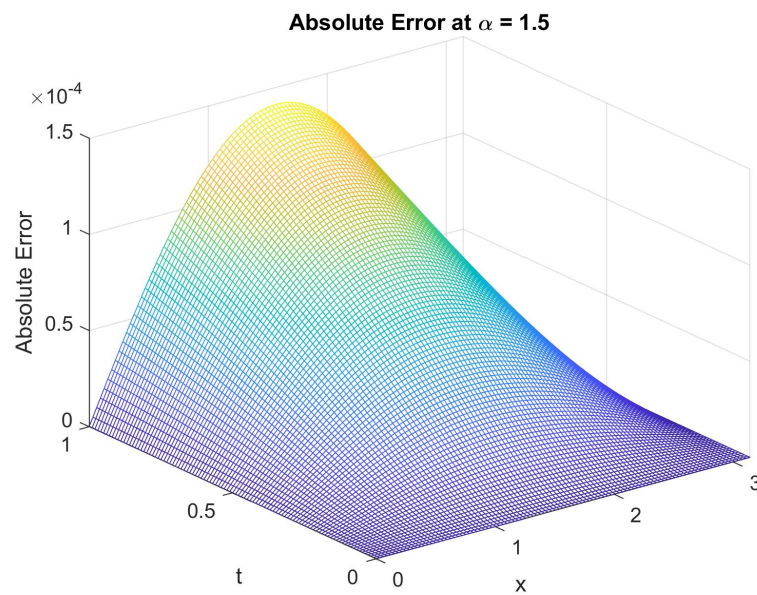


FIGURE 5.8: Graph of the absolute error of Ex. 5.4.2 at  $\alpha = 1.5$ ,  $N_t = 100$ ,  $M_x = 100$ .

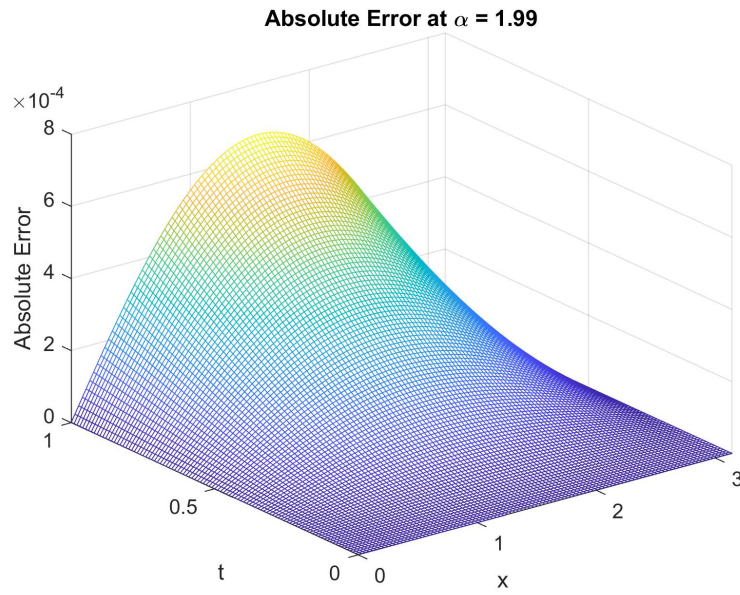


FIGURE 5.9: Graph of the absolute error of Ex. 5.4.2 at  $\alpha = 1.99$ ,  $N_t = 100$ ,  $M_x = 100$ .

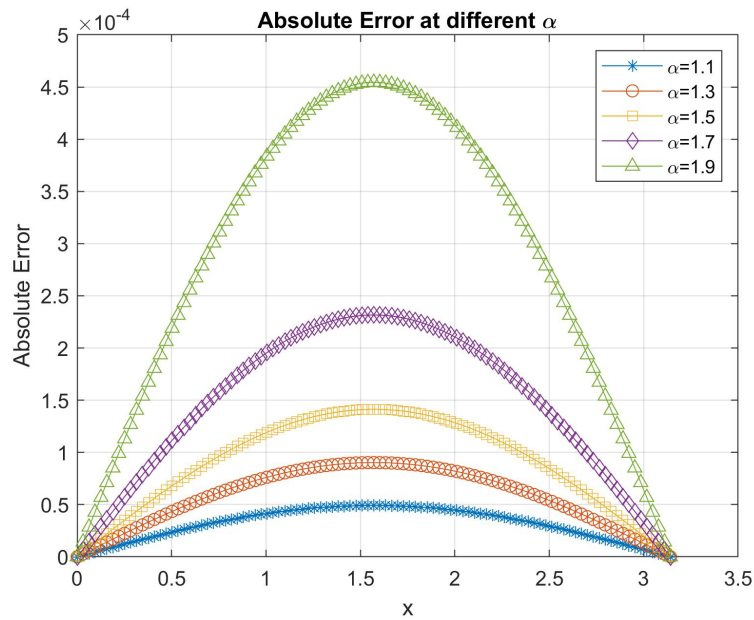


FIGURE 5.10: Graph of the absolute error of Ex. 5.4.2 for different  $\alpha = 1.9$ ,  $N_t = 100$ ,  $M_x = 100$ .

$\alpha$	$\tau$	$L_2$ error		$L_\infty$ error	
		Scheme (5.27)	CO	Scheme (5.27)	CO
<b>1.2</b>	1/8	9.117E-03	-	7.275E-03	-
	1/16	2.432E-03	1.905	1.941E-03	1.906
	1/32	6.552E-04	1.892	5.228E-04	1.892
	1/64	1.756E-04	1.900	1.401E-04	1.900
	1/128	4.672E-05	1.910	3.728E-05	1.910
	1/256	1.239E-05	1.915	9.883E-06	1.915
	1/512	3.325E-06	1.897	2.653E-06	1.897
<b>1.5</b>	1/8	2.675E-02	-	2.134E-02	-
	1/16	6.600E-03	2.019	5.266E-03	2.019
	1/32	1.647E-03	2.003	1.314E-03	2.003
	1/64	4.129E-04	1.996	3.294E-04	1.996
	1/128	1.036E-04	1.994	8.268E-05	1.994
	1/256	2.604E-05	1.992	2.078E-05	1.992
	1/512	6.584E-06	1.984	5.253E-06	1.984
<b>1.99</b>	1/8	1.156E-01	-	9.223E-02	-
	1/16	3.085E-02	1.905	2.462E-02	1.905
	1/32	7.930E-03	1.960	6.327E-03	1.960
	1/64	2.004E-03	1.985	1.599E-03	1.985
	1/128	5.024E-04	1.996	4.008E-04	1.996
	1/256	1.255E-04	2.001	1.001E-04	2.001
	1/512	3.132E-05	2.003	2.499E-05	2.003

TABLE 5.3:  $L_2$  error and  $L_\infty$  error with CO at  $T = 1$ ,  $M_x = 1000$  for Ex. 5.4.2.

$\alpha$	h	$L_2$ error		$L_\infty$ error	
		Scheme (5.27)	CO	Scheme (5.27)	CO
<b>1.2</b>	$\pi/5$	4.814E-03	-	3.653E-03	-
	$\pi/10$	1.213E-03	1.989	9.674E-04	1.917
	$\pi/20$	3.038E-04	1.997	2.424E-04	1.997
	$\pi/40$	7.605E-05	1.998	6.068E-05	1.998
	$\pi/80$	1.909E-05	1.994	1.523E-05	1.994
	$\pi/160$	4.849E-06	1.994	3.869E-06	1.977
<b>1.5</b>	$\pi/5$	3.016E-03	-	2.289E-03	-
	$\pi/10$	7.606E-04	1.987	6.069E-04	1.915
	$\pi/20$	1.907E-04	1.996	1.522E-04	1.996
	$\pi/40$	4.784E-05	1.995	3.817E-05	1.995
	$\pi/80$	1.120E-05	1.983	9.658E-06	1.983
	$\pi/160$	3.169E-06	1.933	2.529E-06	1.933
<b>1.99</b>	$\pi/5$	1.200E-03	-	8.895E-04	-
	$\pi/10$	2.965E-04	1.983	2.366E-04	1.911
	$\pi/20$	7.498E-05	1.984	5.982E-05	1.984
	$\pi/40$	1.943E-05	1.948	1.551E-05	1.948
	$\pi/80$	5.536E-06	1.812	4.417E-06	1.812
	$\pi/160$	2.061E-06	1.425	1.645E-06	1.425

TABLE 5.4:  $L_2$  error,  $L_\infty$  error with CO at  $T = 1$  with  $N_t = 3000$  for Ex. 5.4.2 .

*Example 5.4.3.* Consider the TFTE

$$\begin{cases}
 {}_0^C D_t^\alpha \mathfrak{U}(x, t) + {}_0^C D_t^\beta \mathfrak{U}(x, t) + \mathfrak{U}(x, t) = \frac{\partial^2 \mathfrak{U}(x, t)}{\partial x^2} + f(x, t), & (x, t) \in [-1, 1] \times [0, 1] \\
 I.C. : \mathfrak{U}(x, 0) = \partial_t \mathfrak{U}(x, 0) = 0, & x \in [-1, 1], \\
 B.C. : \mathfrak{U}(l, t) = 0, & l = -1, 1,
 \end{cases}
 \tag{5.33}$$

with the source function

$$f(x, t) = \left( \frac{24t^{4-\alpha}}{\Gamma(5-\alpha)} + \frac{24t^{4-\beta}}{\Gamma(5-\beta)} + t^4 + \pi^2 t^4 \right) \sin(\pi x). \quad (5.34)$$

The exact solution of Ex. 5.4.3 is given by  $\mathfrak{U}(x, t) = t^4 \sin(\pi x)$ . The absolute error in Ex. 5.4.3, for  $\alpha = 1.1, 1.5, 1.9$  are illustrated in Fig. 5.11, 5.12 and 5.13. The absolute error for distinct values of  $\alpha$  at  $T = 1$  can be seen in Fig. 5.14. The CO of the numerical scheme w.r.t.  $x$  and  $t$  for distinct values of  $\alpha$  are provided in Table 5.5-5.6 respectively.

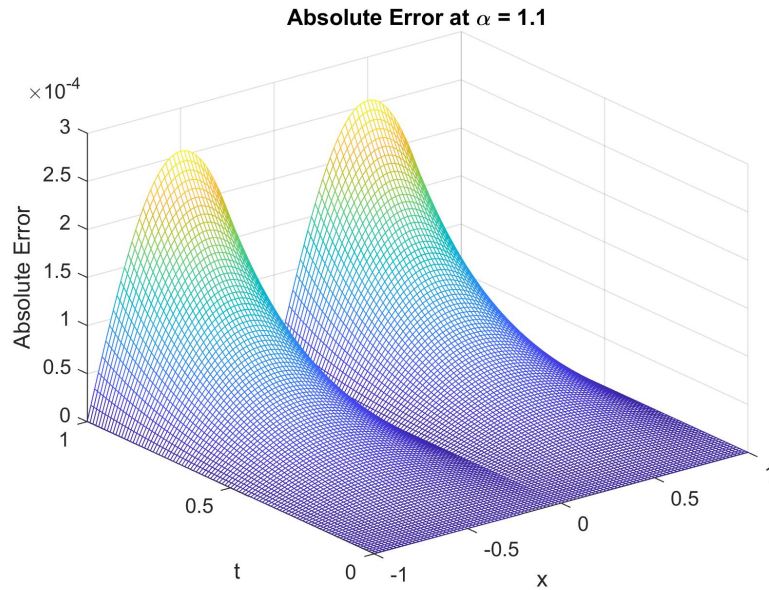


FIGURE 5.11: Graph of the absolute error of Ex. 5.4.3 at  $\alpha = 1.1$ ,  $N_t = 100$ ,  $M_x = 100$ .

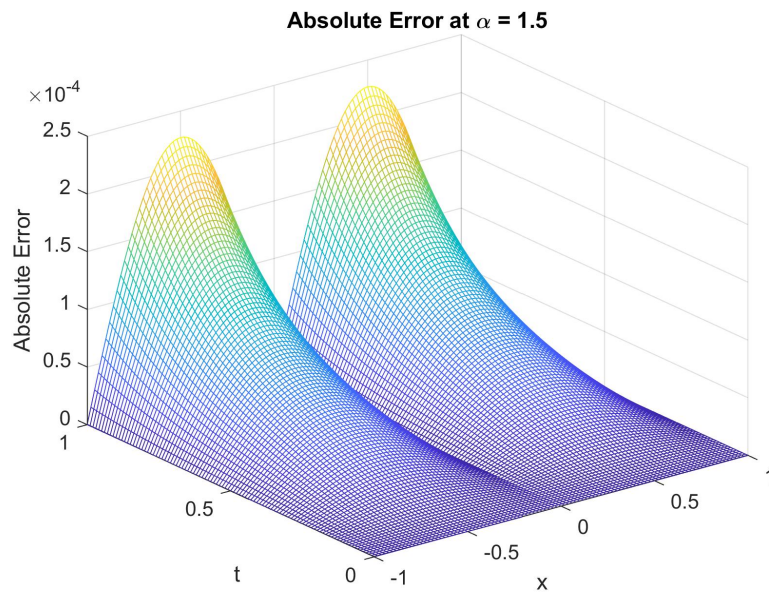


FIGURE 5.12: Graph of the absolute error of Ex. 5.4.3 at  $\alpha = 1.5$ ,  $N_t = 100$ ,  $M_x = 100$ .

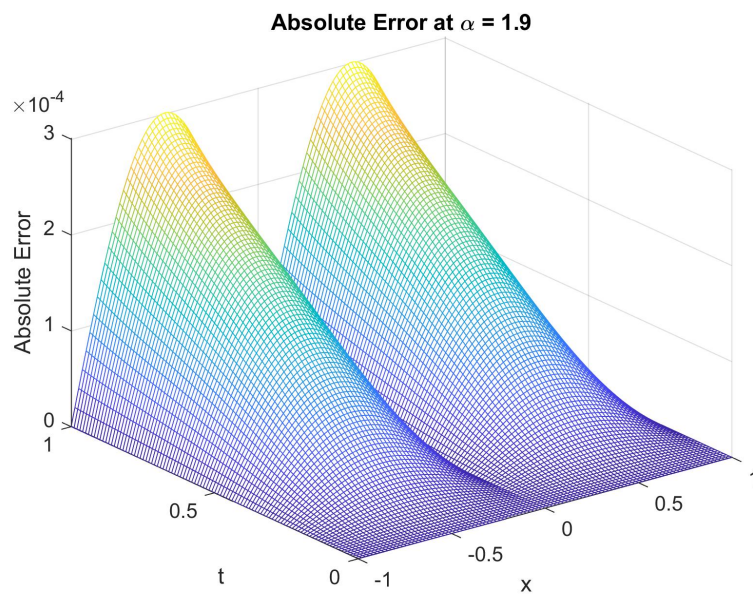


FIGURE 5.13: Graph of the absolute error of Ex. 5.4.3 at  $\alpha = 1.9$ ,  $N_t = 100$ ,  $M_x = 100$ .

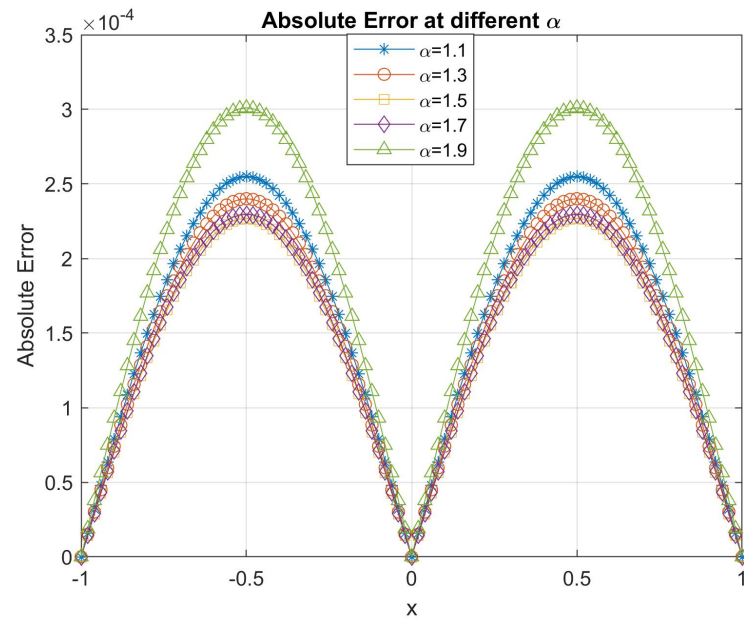


FIGURE 5.14: Graph of the absolute error of Ex. 5.4.3 for different  $\alpha$ ,  $N_t = 100$ ,  $M_x = 100$ .

$\alpha$	$\tau$	$L_2$ error		$L_\infty$ error	
		Scheme (5.27)	CO	Scheme (5.27)	CO
<b>1.1</b>	1/10	5.636E-03	-	5.636E-03	-
	1/20	1.518E-03	1.893	1.518E-03	1.893
	1/40	3.941E-04	1.945	3.941E-04	1.945
	1/80	1.016E-04	1.956	1.016E-04	1.956
	1/160	2.703E-05	1.910	2.703E-05	1.910
	1/320	8.214E-06	1.718	8.214E-06	1.718
	1/640	3.488E-06	1.236	3.488E-06	1.236
<b>1.5</b>	1/10	9.018E-03	-	9.018E-03	-
	1/20	2.193E-03	2.040	2.193E-03	2.040
	1/40	5.357E-04	2.033	5.357E-04	2.033
	1/80	1.322E-04	2.019	1.322E-04	2.019
	1/160	3.357E-05	1.977	3.357E-05	1.977
	1/320	9.364E-06	1.842	9.364E-06	1.842
	1/640	3.398E-06	1.462	3.398E-06	1.462
<b>1.9</b>	1/10	2.383E-02	-	2.383E-02	-
	1/20	5.762E-03	2.048	5.762E-03	2.048
	1/40	1.380E-03	2.062	1.380E-03	2.062
	1/80	3.323E-04	2.054	3.323E-04	2.054
	1/160	8.083E-05	2.040	8.083E-05	2.040
	1/320	2.023E-05	1.998	2.023E-05	1.998
	1/640	5.592E-06	1.855	5.592E-06	1.855

TABLE 5.5:  $L_2$  error and  $L_\infty$  error with CO for Ex. 5.4.3 at  $T = 1$  with  $M_x = 1000$ .

$\alpha$	h	$L_2$ error		$L_\infty$ error	
		Scheme (5.27)	CO	Scheme (5.27)	CO
<b>1.1</b>	2/5	7.792E-02	-	7.410E-02	-
	2/10	1.919E-02	2.021	1.825E-02	2.021
	2/20	4.779E-03	2.006	4.779E-03	1.933
	2/40	1.194E-03	2.001	1.194E-03	2.001
	2/80	2.985E-04	2.000	2.989E-04	2.000
	2/160	7.473E-05	1.998	7.473E-05	1.998
	2/320	1.880E-05	1.991	1.880E-05	1.991
<b>1.5</b>	2/5	5.721E-02	-	5.441E-02	-
	2/10	1.435E-02	1.995	1.365E-02	1.995
	2/20	3.590E-03	1.999	3.590E-03	1.927
	2/40	8.978E-04	2.000	8.978E-04	2.000
	2/80	2.246E-04	1.999	2.246E-04	1.999
	2/160	5.630E-05	1.996	5.630E-05	1.996
	2/320	1.422E-05	1.985	1.422E-05	1.985
<b>1.9</b>	2/5	3.550E-02	-	3.377E-02	-
	2/10	9.071E-03	1.969	8.627E-03	1.969
	2/20	2.280E-03	1.992	2.280E-03	1.920
	2/40	5.711E-04	1.997	5.711E-04	1.997
	2/80	1.432E-04	1.996	1.432E-04	1.996
	2/160	3.613E-05	1.936	3.613E-05	1.986
	2/320	9.376E-06	1.946	9.376E-06	1.946

TABLE 5.6:  $L_2$  error,  $L_\infty$  error with CO for Ex. 5.4.3 at  $T = 1$  with  $N_t = 2000$ .

*Example 5.4.4.* Consider the TFTE

$$\begin{cases} {}_0^C D_t^\alpha \mathfrak{U}(x, t) + {}_0^C D_t^\beta \mathfrak{U}(x, t) + \mathfrak{U}(x, t) = \frac{\partial^2 \mathfrak{U}(x, t)}{\partial x^2} + f(x, t), & (x, t) \in [-1, 1] \times [0, 1] \\ I.C. : \mathfrak{U}(x, 0) = \partial_t \mathfrak{U}(x, 0) = 0, & x \in [-1, 1], \\ B.C. : \mathfrak{U}(l, t) = \frac{t^4}{e}, & l = -1, 1, \end{cases} \quad (5.35)$$

with the source function

$$f(x, t) = \left( \frac{24t^{4-\alpha}}{\Gamma(5-\alpha)} + \frac{24t^{4-\beta}}{\Gamma(5-\beta)} + t^4 - (4x^2 - 2)t^4 \right) e^{-x^2}. \quad (5.36)$$

The exact solution of Ex. 5.4.4 is  $\mathfrak{U}(x, t) = t^4 e^{-x^2}$ . The absolute error in Ex. 5.4.4, for  $\alpha = \{1.1, 1.5, 1.9\}$  are shown in Fig. 5.15, 5.16 and 5.17. The absolute error for different value of  $\alpha$  are shown in Fig. 5.18. Table 5.7-5.8 shows the CO of the numerical scheme for distinct values of  $\alpha$ .

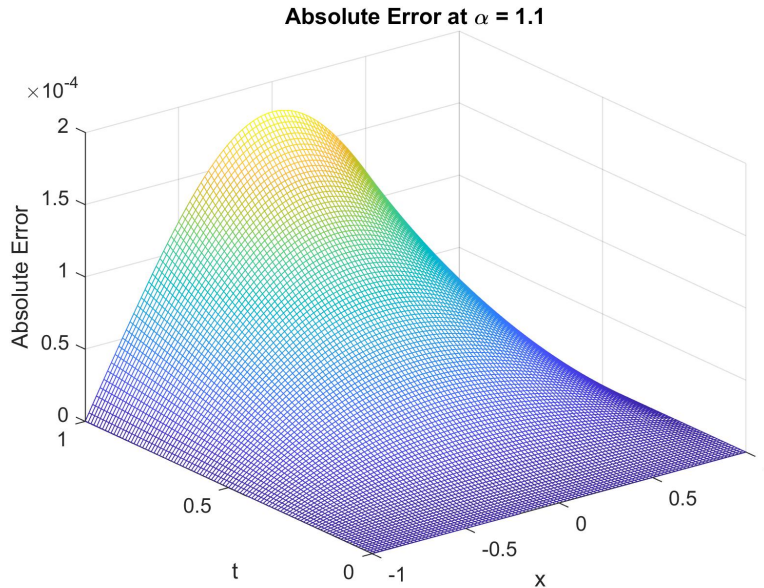


FIGURE 5.15: Graph of the absolute error of Ex. 5.4.4 at  $\alpha = 1.1$ ,  $N_t = 100$ ,  $M_x = 100$ .

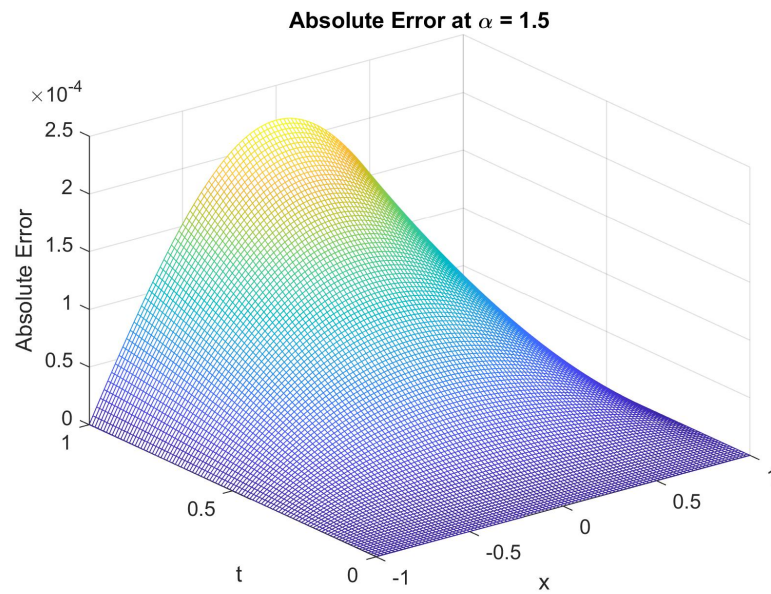


FIGURE 5.16: Graph of the absolute error of Ex. 5.4.4 at  $\alpha = 1.5$ ,  $N_t = 100$ ,  $M_x = 100$ .

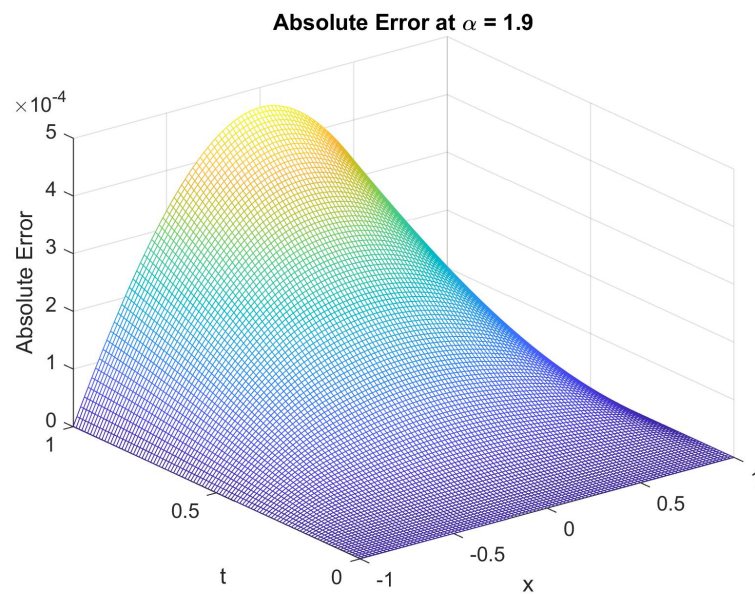


FIGURE 5.17: Graph of the absolute error of Ex. 5.4.4 at  $\alpha = 1.9$ ,  $N_t = 100$ ,  $M_x = 100$ .

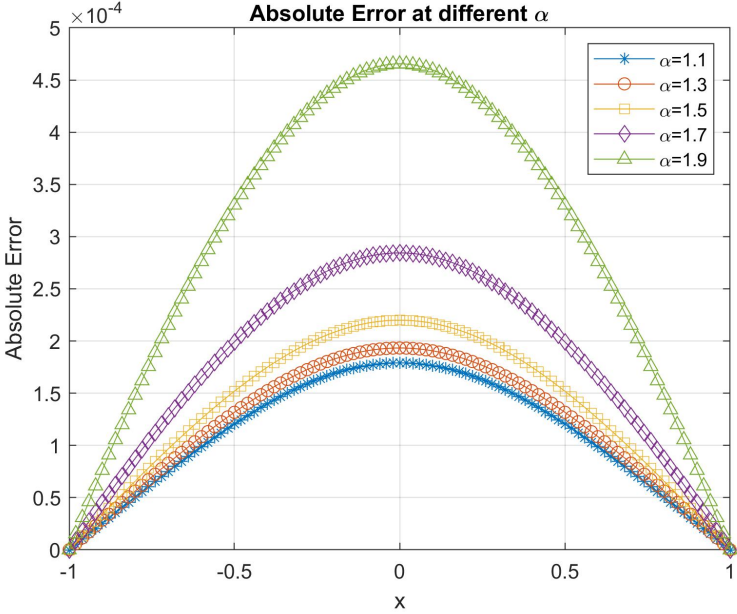


FIGURE 5.18: Graph of the absolute error of Ex. 5.4.4 for different  $\alpha$ ,  $N_t = 100$ ,  $M_x = 100$ .

$\alpha$	$\tau$	$L_2$ error		$L_\infty$ error	
		Scheme (5.27)	CO	Scheme (5.27)	CO
<b>1.1</b>	1/10	1.314E-02	-	1.285E-02	-
	1/20	3.614E-03	1.863	3.534E-03	1.862
	1/40	9.440E-04	1.937	9.223E-04	1.936
	1/80	2.411E-04	1.969	2.359E-04	1.969
	1/160	6.102E-05	1.982	5.987E-05	1.981
	1/320	1.548E-05	1.979	1.522E-05	1.973
	1/640	4.028E-06	1.942	4.022E-06	1.920
<b>1.5</b>	1/10	2.091E-02	-	2.048E-02	-
	1/20	5.300E-03	1.980	5.194E-03	1.979
	1/40	1.312E-03	2.014	1.286E-03	2.014
	1/80	3.228E-04	2.023	3.165E-04	2.023
	1/160	7.948E-05	2.022	7.797E-05	2.021
	1/320	1.968E-05	2.014	1.936E-05	2.010
	1/640	4.954E-06	1.990	4.924E-06	1.975
<b>1.9</b>	1/10	4.725E-02	-	4.618E-02	-
	1/20	1.203E-02	1.974	1.182E-02	1.966
	1/40	2.971E-03	2.018	2.930E-03	2.013
	1/80	7.252E-04	2.034	7.160E-04	2.033
	1/160	1.762E-04	2.041	1.741E-04	2.040
	1/320	4.279E-05	2.042	4.231E-05	2.041
	1/640	1.042E-05	2.037	1.034E-05	2.032

TABLE 5.7:  $L_2$  error and  $L_\infty$  error with CO for Ex. 5.4.4 at  $T = 1$  with  $M_x = 1000$ .

$\alpha$	h	$L_2$ error		$L_\infty$ error	
		Scheme (5.27)	CO	Scheme (5.27)	CO
<b>1.1</b>	2/5	1.020E-02	-	1.118E-02	-
	2/10	2.505E-03	2.025	3.148E-03	1.828
	2/20	6.232E-04	2.007	7.824E-04	2.008
	2/40	1.556E-04	2.002	1.953E-04	2.002
	2/80	3.891E-05	2.000	4.884E-05	2.000
	2/160	9.784E-06	1.997	1.223E-05	1.998
	2/320	2.458E-06	1.988	3.080E-06	1.990
<b>1.5</b>	2/5	7.114E-03	-	7.916E-03	-
	2/10	1.766E-03	2.011	2.297E-03	1.785
	2/20	4.400E-04	2.005	5.720E-04	2.005
	2/40	1.099E-04	2.001	1.429E-04	2.001
	2/80	2.749E-05	1.999	3.574E-05	1.999
	2/160	6.896E-06	1.995	8.959E-06	1.996
	2/320	1.747E-05	1.981	2.265E-06	1.984
<b>1.9</b>	2/5	4.524E-03	-	5.054E-03	-
	2/10	1.153E-03	1.972	1.532E-03	1.722
	2/20	2.890E-04	1.996	3.838E-04	1.997
	2/40	7.224E-05	1.996	9.620E-05	1.996
	2/80	1.828E-05	1.987	2.427E-05	1.987
	2/160	4.741E-06	1.947	6.280E-06	1.950
	2/320	1.362E-06	1.800	1.784E-06	1.816

TABLE 5.8:  $L_2$  error,  $L_\infty$  error with CO for Ex. 5.4.4 at  $T = 1$  with  $N_t = 2000$ .

## 5.5 Conclusion

In summary, we have proposed a novel difference scheme to solve TFTE. The Caputo fractional derivatives of order  $\alpha \in (1,2)$  and  $\beta \in (0,1)$  have been approximated by L3 and L123 approximation respectively, whereas spatial derivatives have been approximated by central difference scheme. The numerical scheme is validated on four numerical examples and the obtained results are highly accurate and of second order w.r.t.  $x$  and  $t$ . The comparative study of the numerical results with [3] in Table 5.1 proves the effectiveness of our scheme. The proposed approach can be extended for the nonlinear and higher dimensional TFWE in future.

\*\*\*\*\*

